Acetonitrile-Based Highly Concentrated Electrolytes for High-Power Organic Sodium-Ion Batteries

Yoshiyuki Gambe,[a] Hiroaki Kobayashi,[b]* and Itaru Honma[a]*

[a]Institute of Multidisciplinary Research for Advanced Materials, Tohoku University, 2-1-1 Katahira, Aoba-ku, Sendai, Miyagi, 980-8577, Japan.

[b]Department of Chemistry, Faculty of Science, Hokkaido University, Kita 10, Nishi 8, Kita-ku, Sapporo, Hokkaido, 060-0810, Japan.

KEYWORDS: Highly concentrated electrolytes, Acetonitrile, Organic sodium-ion batteries, High voltage cathodes, Sodium croconate molecules

ABSTRACT: Sodium croconate, a high-voltage organic cathode material, can be applied to high-energy-density and cost-effective organic sodium-ion batteries (OSIBs) as an alternative to traditional lithium-ion batteries. However, organic molecular cathodes generally dissolve into the electrolyte, leading to poor cyclability. Thus, an electrolyte that can address the present limitations and further the fabrication of highly reversible OSIBs must be developed. To address this gap in the literature, in this study, we demonstrate an acetonitrile (AN)-based highly concentrated electrolyte (HCE) with sodium bis(fluorosulfonyl)imide (NaFSI). This electrolyte has an ionic conductivity of 12.1 mS cm^{-1}, which is higher than those of previously reported HCEs. Moreover, the developed HCE (NaFSI:AN molar ratio = 1:2.7) exhibits a high Na^+ transference number of 0.49. A full-cell OSIB bearing this electrolyte demonstrates high-power operation with improved capacity retention. The solvent-free electrolyte with the solvation structure of the [$2Na^+$-FSI^-] aggregate suppresses the dissolution of organic molecules, leading to their high performance.

INTRODUCTION

Lithium-ion batteries (LIBs) are the main energy storage systems used in many applications such as smartphones, laptops, drones, and electric vehicles.[1,2] However, the rapid increase in the demand for these batteries has led to a limited supply of resources such as lithium and cobalt.[3] Organic sodium-ion batteries (OSIBs) prepared with organic cathode materials have recently been developed as an alternative to traditional LIBs. Sodium resources are more abundant in the Earth's crust than lithium resources, and organic molecules are usually composed of light elements (C, O, H, N, etc.) obtained from industrial chemicals and biomass.[4,5] OSIBs can be used to develop completely precious-metal-free and environmentally friendly secondary batteries.

Organic cathode materials for LIBs and SIBs can be categorized as small molecules,[6,7,16–22,8–15] polymers,[23–29] sulfur-based materials,[29–31] and radicals.[23,32] The main strategy for improving battery performance is to design an organic electrode structure; in this context, the correlation between the electrode structure and battery performance has been evaluated. However, OSIBs, especially those prepared from small organic molecules, undergo extensive dissolution into the electrolyte, leading to cycling degradation. Therefore, both the electrode and electrolyte should be well-designed for high-performance OSIBs.

Highly concentrated electrolytes (HCEs) are a hot topic in the development of energy storage systems owing to their unique features, which include high electrolyte/electrode interphase stability, Al foil corrosion suppression, wide electrochemical window, and high ion transference property.[33] Dokko *et al*. revealed that a sulfolane-based HCE prepared with sodium bis(fluorosulfonyl)imide (NaFSI) salt demonstrated a unique Na^+ hopping conduction mechanism, with a Na^+ transference number (t_{Na+}) as high as 0.8.[34] Yamada's research group applied a succinonitrile-based HCE with NaFSI to a hard carbon anode to prepare SIBs; the authors observed solid electrolyte interphase (SEI) formation derived from the FSI^- anion at ultrahigh concentrations.[35] In addition, it was revealed that a localized HCE diluted with a low-polarity cosolvent indicated high ionic conductivity and less-flammable feature.[36–39] HCEs have also been applied to OSIBs; the dissolution of organic molecules can be suppressed by limiting the presence of non-coordinated (free) solvent molecules in HCEs. For example, Chen *et al*. reported that increasing $NaSO_3CF_3$ salt concentration in triglyme decreased the solubility of 9, 10-anthraquinone, resulting in better cycling performance.[40] However, increasing the salt concentration would also increase the viscosity of the electrolyte, leading to low ionic conductivity and poor rate capability at room temperature. Thus, the development of an HCE with high ionic conductivity is a necessary undertaking toward high-power OSIBs.

Herein, we demonstrate the acetonitrile (AN)-based HCE with NaFSI having a unique ion transport property. NaFSI can be dissolved in suitable solvents at high concentration (>5 M) owing to its low cation-anion interaction. AN solvent is known to have lower viscosity than other solvents,[41] high dielectric constant, and relatively high oxidative stability.

From the above points, to develop the HCE having higher ion transport properties, we chose NaFSI/AN-based electrolytes and evaluated the transport properties. We also study the relationship between the battery performance of OSIBs with a sodium croconate ($C_5O_5Na_2$) cathode and the solution structure of NaFSI/AN-based HCE. The croconate molecule is a promising high-voltage (4 V vs. Li, 3.5 V vs. Na) organic cathode material for LIBs[13] and SIBs.[22] However, the fully oxidized form of this molecule, cyclopentanepentone (C_5O_5), dissolves into the electrolyte, leading to poor cyclability; in addition, its intermediate, the sodium croconate radical, dimerizes, further inducing C_5O_5 molecule decomposition (see Fig. 1).[22] We selected the $C_5O_5Na_2$ cathode to evaluate the correlation between the solution structure of HCE and battery performances. We fabricated the OSIBs with $C_5O_5Na_2$ cathode and NaFSI/AN-based electrolytes and evaluated the battery performance and the correlation with the solution structure of the developed electrolytes.

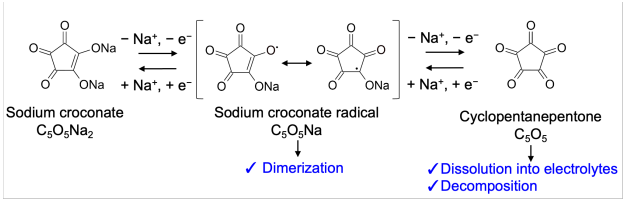

Figure 1. Proposed two-electron redox reactions of $C_5O_5Na_2$ molecules during charging/discharging at 3.5 V vs. Na/Na^+ and estimated cycling degradation mechanism of a $C_5O_5Na_2$-based organic sodium-ion battery with an organic liquid electrolyte.

EXPERIMENTAL SECTION

Materials. NaFSI powder (99%, Kishida Chemicals Co., Ltd.), sodium hexafluorophosphate ($NaPF_6$, 99%, Kishida Chemicals Co., Ltd.), AN (99.5%, Kanto Chemical Co., Inc.), 1,2-dimethoxyethane (DME, 99.5%, Kanto Chemical Co., Inc.), and propylene carbonate (PC, 98.0%, FUJIFILM Wako Chemicals Co.,) were used to prepare the electrolytes. The electrolytes were prepared by dissolving the NaFSI powder in AN at NaFSI:AN molar ratios of 1:1, 1:2, 1:2.7, 1:8, or 1:20 in sealed glass vials. The concentrated solutions (NaFSI:AN molar ratios = 1:1–1:2.7) were heated at 50 °C to completely dissolve the NaFSI salt. $C_5O_5Na_2$ (97%, Sigma-Aldrich Co.), COOH-MWCNT (COOH functionalized: >8%, average diameter: 9.5 nm, length: 1.5 μm, Sigma-Aldrich Co.), and polytetrafluoroethylene (PTFE, Teflon-6J, DuPont-Mitsui Fluorochemicals Co., Ltd.) were used to fabricate the cathode composite sheets. Hard carbon (Kuranode® type2: 5 μm) was provided by Kuraray Co., Ltd., and used as an anode. Polyvinylidene difluoride (PVDF, KF 1100, KUREHA) was used as the binder for the anode sheet.

Characterizations. Ionic conductivity was evaluated by two-probe AC impedance spectroscopy in a symmetric cell (SUS | electrolyte | SUS) using a CellTest system (Solartron, 1470E, 1400A). The temperature dependence of the ionic conductivity of the electrolytes was evaluated in the range of 10–60°C. The viscosities of the electrolytes were measured using a Brookfield viscometer (DV2T; LV). A symmetric cell [Na metal | electrolyte | Na metal] was fabricated in an Ar-filled glove box to evaluate the t_{Na+} of the electrolytes. Na-metal foil was cut into discs (diameter = 16 mm) and four sheets of a separator (Celgard 3501, thickness = 25 μm, diameter = 16 mm) were inserted between the two Na-metal electrodes in a 2032-type coin cell. The electrolytes (100 μL) were soaked into the separator. After the open-circuit-voltage of the Na symmetric cell is stable, electrochemical polarization (ΔV = 10 mV) and AC impedance measurements were performed at 25 °C using a CellTest system. AC impedance measurements were conducted before and after electrochemical polarization in the frequency range of 1 MHz–100 mHz, with an AC amplitude of 10 mV. The solution structure was evaluated by Raman spectroscopy using an XploRA spectrometer (excitation wavelength = 532 nm; HORIBA). The samples were placed in a quartz cell and sealed with vacuum grease in an Ar-filled glove box. The spectra were deconvoluted using a Gaussian–Lorentzian function with a linear background. Elemental compositions and chemical states of SEI on hard carbon anode after first charge/discharge measurement were investigated by X-ray photoelectron spectroscopy (XPS, PHI5000, VersaProbe II, monochromatic Al Kα source ($h\upsilon$ = 1486.6 eV)). Coin cells of $C_5O_5Na_2$/hard carbon full-cell after first charge/discharge were disassembled in Ar-filled glove box, and the hard carbon anodes were prepared by washing five times with dimethyl carbonate (DMC) and drying at room temperature under vacuum. The samples were transferred to the XPS chamber without exposure to air. Chemical structure of organic molecules dissolved into the electrolyte was evaluated by ^{13}C nuclear magnetic resonance (NMR, AVANCE IV 500 MHz, Bruker Biospin).

Battery Performance of $C_5O_5Na_2$ Cathode/Hard Carbon Anode Cells. A cathode sheet was prepared by mixing the $C_5O_5Na_2$ (23.7 wt%), COOH-MWCNT (71.3 wt%), and PTFE (5.0 wt%) using an agate mortar and pestle. The cathode sheet (5 mg, diameter = 7 mm) was prepared. The COOH-MWCNT carbon material was used for the formation of hydrogen bonding between COOH functional groups on MWCNT and carbonyl groups (C=O) in $C_5O_5Na_2$ molecules, improving the cycling performance as reported in our recent research.[22] An anode slurry was prepared by mixing hard carbon (90 wt%), PVDF (10 wt%) and *N*-methylpyrrolidone as a solvent using a planetary centrifugal mixer (AR-100 Conditioning Mixer, Thinky). The prepared slurry was coated on Al foil as the current collector and dried overnight at 120 °C under vacuum. The mass loading of the active materials was approximately 2–3 mg cm^{-2}. A cell was fabricated by stacking the $C_5O_5Na_2$ cathode sheet, a glass fiber (GA55, ADVANTEC) or Celgard3401 as the separator, and the hard carbon anode sheet in a CR2032-type coin cell in an Ar-filled glove box. The electrolytes (40 μL) were soaked into the separator. A carbon-coated Al foil (diameter = 16 mm) was inserted between the $C_5O_5Na_2$ cathode sheet and coin-cell cap (SUS) to suppress the corrosion of the SUS. The capacity of the negative electrode to the positive electrode (N/P ratio) was fixed at 1.2–1.4. The specific capacities of the cells were calculated based on the mass of $C_5O_5Na_2$ in the cathode composite sheet. The charge/discharge measurements were carried out at 25°C and C-rates of 0.2–10 C in the cut-off voltage range of 2.5–4.0 V.

RESULTS AND DISCUSSION

Ion Transport Property. Electrolyte solutions with NaFSI:AN molar ratios of 1:1, 1:2, 1:2.7, 1:8, and 1:20 were prepared by mixing NaFSI and AN (Fig. 2a) in sealed vials until a transparent homogeneous solution was obtained.

The most concentrated electrolyte (NaFSI:AN molar ratio = 1:1, see Fig. 2b) and all other electrolytes maintained a liquid state at room temperature. The salt concentration in electrolytes with NaFSI:AN molar ratios = 1:1, 1:2, and 1:2.7 exceeded 4.5 M; thus, they were evaluated as HCEs. The ion transport property of the AN-based electrolytes was investigated by evaluating their ionic conductivity using two-probe AC impedance measurement over the temperature ranges of 10–60 °C (see Fig. 2c). Although their ionic conductivity decreased with increasing salt concentration, the electrolytes with NaFSI:AN molar ratios = 1:2 and 1:2.7 showed good ionic conductivities as high as 6.3 and 12.1 mS cm^{-1} , respectively, at 25 °C; these values are higher than those of HCEs for SIBs reported in previous studies.[35,42,43] The viscosity of AN (0.3 cP at 25°C) is lower than that of solvents generally used in SIBs (summarized in Table S1), such as propylene carbonate (PC, 2.53 cP at 25°C);[41] thus, it could maintain the low viscosity of electrolytes with salt concentrations higher than 4.5 M (see Table 1). Among the electrolytes investigated, that with the highest salt concentration (NaFSI:AN molar ratio =1:1) showed the highest viscosity, leading to its low ionic conductivity (0.8 mS cm^{-1} at 25°C). The Arrhenius plot of the ionic conductivity of the electrolytes can be fitted by the Vogel–Fulcher–Tamman (VFT) equation (eq 1):[44]

$$\sigma = \sigma_0 \, exp\left(\frac{-B}{T - T_0}\right) \qquad (1)$$

where σ_0 (S cm^{-1}), B (K), and T_0 (K) are constants. The fitted parameters are listed in Table S2. B, which is the apparent activation energy, ranged from 300 to 400 in the HCEs with NaFSI:AN molar ratios of 1:2 and 1:2.7; these values are comparable with those of 1 M $NaPF_6$ carbonate-based electrolyte generally used in SIBs.[44] The B of the electrolyte with a NaFSI:AN molar ratio of 1:1 increased to 618, which is close to those of ionic liquids and glyme complex electrolytes, which are HCE well studied in LIBs.[45]

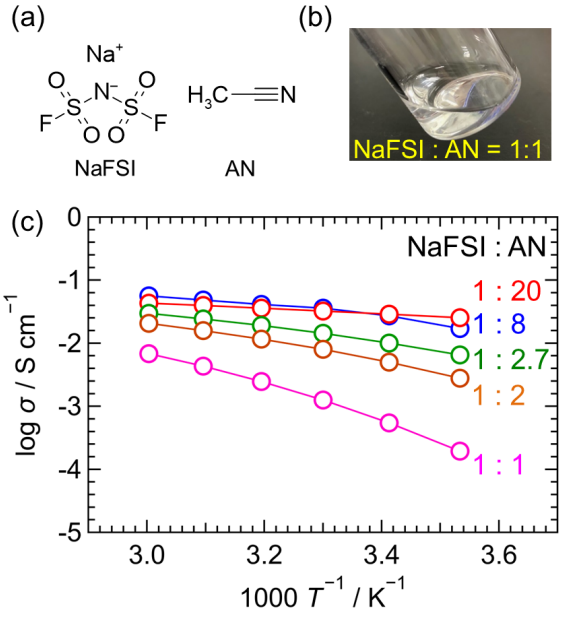

Figure 2. (a) Chemical structures of NaFSI and AN. (b) Photograph of a highly concentrated electrolyte (NaFSI:AN molar ratio = 1:1). (c) Arrhenius plots of the ionic conductivity of the NaFSI/AN-based electrolytes (NaFSI:AN molar ratios = 1:1, 1:2, 1:2.7, 1:8, and 1:20).

Table 1. Ionic conductivities, viscosities, and transference numbers of the NaFSI/AN-based electrolytes at 25 °C.

NaFSI:AN molar ratio	σ / mS cm^{-1}	Viscosity / c P	t_{Na+}
1:20	30.1	0.7	-
1:8	28.5	1.7	-
1:2.7	12.1	11.9	0.49
1:2	6.3	36.56	0.50
1:1	0.8	582.9	-

To further investigate the Na-ion transport properties of the electrolytes, we evaluated the t_{Na+} of a Na symmetric cell with the AN-based electrolytes (NaFSI:AN molar ratio = 1:2.7) using potentiostatic polarization (ΔV = 10 mV) and AC impedance measurements (see Fig. 3). As shown in Fig. 3a, immediately after the application of a DC voltage of 10 mV, an initial current (I_0) 19.3 μA was recorded. Subsequently, the current sharply decreased and stabilized from approximately 100 to 600 s, implying that there is fewer side reactions within this time scale and applied voltage. The steady-state current was 15.8 μA. The Nyquist plots obtained before and after the applied voltage were basically identical, and interface resistance and concentration polarization were observed at frequencies of 100 kHz–10 Hz and lower than 10 Hz, respectively (see Fig. 3b, c). These results revealed minimal concentration polarization and a rapid frequency response. The interface resistance includes the charge transfer resistance at the Na-metal electrode and the resistance of the passivation layers; SEI at Na-metal surface. t_{Na+} was estimated using the following equation (eq 2):[46]

$$t_{Na^+} = \frac{I_{ss}(\Delta V - I_0 R_{i,0})}{I_0(\Delta V - I_{ss} R_{i,ss})} \qquad (2)$$

where ΔV, I_0, and I_{ss} are the applied voltage, initial current, and steady-state current, respectively, and $R_{i,0}$, and $R_{i,SS}$ are the interfacial resistances before and after potentiostatic polarization, respectively. The detailed parameters are summarized in Table S3. The t_{Na+} value of the electrolyte with a NaFSI:AN molar ratio of 1:2.7 was estimated to be 0.49, which is higher than that of traditional carbonate-based electrolytes. The t_{Na+} value of the electrolyte with a NaFSI:AN molar ratio of 1:2 electrolyte was as high as 0.50 (see Table 1 and Fig. S1). In previous studies,[47] it was reported that HCEs exhibit a large t_{Na+}; however, increases in their viscosity are disadvantageous to their ionic conductivities (see Table S3). By contrast, the AN-based HCE (NaFSI:AN molar ratio = 1:2.7) developed in this study achieved both high ionic conductivity (12.1 mS cm^{-1}) and t_{Na+} (0.49).

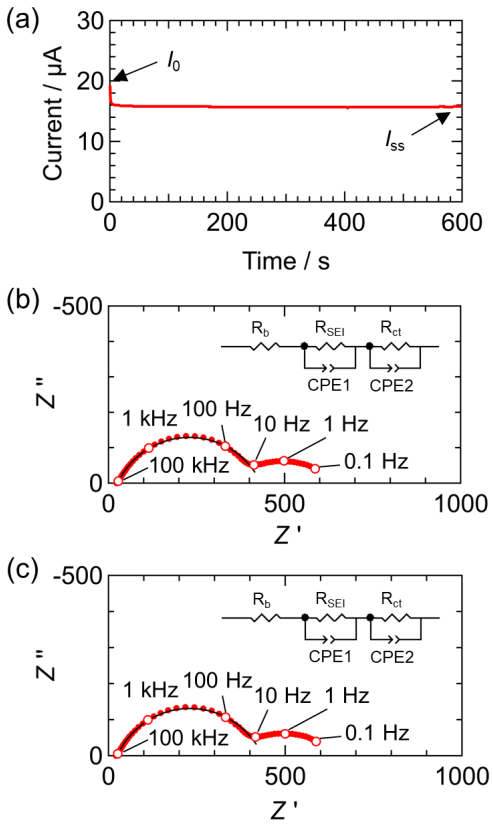

Figure 3. (a) Chronoamperogram of the Na symmetric cell [Na metal | NaFSI:AN = 1:2.7, molar ratio | Na metal] at a constant voltage of 10 mV. Nyquist plots of the cell in the frequency range of 1 MHz–0.1 Hz (b) before and (c) after the polarization measurements. Red points and black solid lines indicate the experimental and fitting data obtained in the frequency range of 100kHz–10Hz, respectively.

Solution Structure. To investigate the solution structure of the AN-based HCE, the coordination state of the AN solvent was analyzed using Raman spectra (see Fig. 4a). The band at approximately 2246 cm^{-1} was assigned to the C≡N bond of AN solvent[48] and shifted toward higher wavenumbers with increasing NaFSI salts concentration; this result indicates that the C≡N bonds are coordinated to a Na^+ cation.[35,49] At higher NaFSI salt concentrations (NaFSI:AN molar ratio = 1:2.7–1:1), nearly all C≡N bonds were coordinated with Na^+ cations, indicating a lack of free (noncoordinated) C≡N bonds. A thermogravimetric analysis of the electrolytes is also shown in Fig. S2. The thermal stability of the electrolyte with a NaFSI:AN molar ratio of 1:1 was drastically improved compared with that of free AN solvent because of the lower amount of free-AN molecules available in the electrolyte.

In addition, the coordination states of the FSI^- anion changed with increasing NaFSI salt concentration (see Fig. 4b). The vibrational modes of FSI^- were observed in the range of 720–750 cm^{-1}. The Raman spectra of the electrolytes were deconvoluted into four peaks at approximately 724, 734, 744, and 750 cm^{-1}, which can be assigned to free FSI anions, contact ion pairs (CIPs, FSI^- anion coordinating to one Na^+), aggregates-I (AGG-I, FSI^- anion coordinating to two Na^+), and aggregates-II (AGG-II, FSI^- anion coordinating to three Na^+), respectively. Increases in NaFSI salt concentration resulted in a decrease in the peaks of free FSI^- and increase in the peaks of the AGG-I. In the most concentrated solution (NaFSI:AN molar ratio = 1:1), the FSI^- anions existed solely as AGG-II structures, which is in agreement with previous reports.[35] To study the correlation between the above solvate structure of the AN-based HCEs and battery performance, we performed charge/discharge measurements of OSIBs prepared with the developed HCEs in the following section.

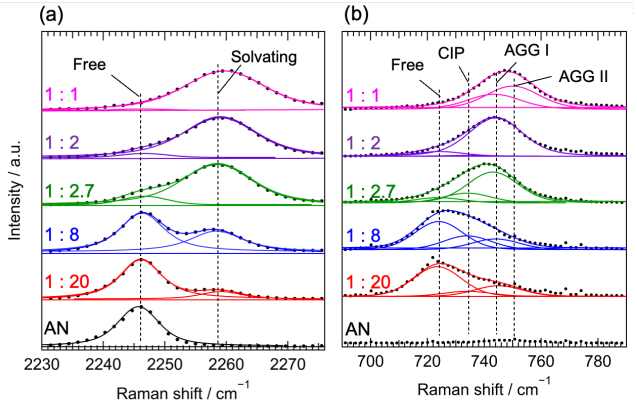

Figure 4. Raman spectra of the AN-based electrolytes (NaFSI:AN molar ratios = 1:1, 1:2, 1:2.7, 1:8, and 1:20) in the range of (a) 2230–2276 cm^{-1} (C≡N stretching mode of AN) and (b) 690–790 cm^{-1} (vibrational mode of FSI^-) at room temperature. Black points and solid lines indicate the experimental spectra and fitting curves, respectively.

Charge/Discharge Profiles. First, we evaluated the performance of a half-cell with a $C_5O_5Na_2$ cathode, the AN-based electrolyte, and a Na-metal anode. However, a side reaction occurred at the Na-metal anode during charging, rendering the operation of the battery cell difficult even under highly concentrated conditions (see Fig. S3). Therefore, in this study, we evaluated the performance of a full-cell configuration with a $C_5O_5Na_2$ cathode, the AN-based electrolytes, and a hard carbon anode. The first charge/discharge profiles of the OSIBs are shown in Fig. 5a. The profiles of the cells with the AN-based electrolytes (NaFSI:AN molar ratios = 1:1, 1:2, 1:2.7, and 1:8) were consistent with those in our previous report. [22] Moreover, the dQ/dV plots (see Fig. S4) for the AN-based HCEs (NaFSI:AN molar ratios = 1:8, 1:2.7, and 1:2) clearly revealed the redox reaction of $C_5O_5Na_2$/hard carbon at approximately 3.5–3.7 V; this finding is comparable with the results of $C_5O_5Na_2$/hard carbon full-cells with carbonate-based electrolytes (see Fig. S5), indicating the successful redox reaction of the $C_5O_5Na_2$ cathode/hard carbon anode with AN-based HCEs. Note that the broad peaks appearing at approximately 2.5–3.0 V during the first charging cycle are attributable to SEI formation (see Fig. S4). However, in the first charge profile of the cell with the electrolyte with a NaFSI:AN molar ratio of 1:20, a side reaction was observed at approximately 3 V (see Fig. S4), and the first discharge capacity was 47 mAh g^{-1}, indicating that the electrolyte had decomposed at the hard carbon anode interface; hence, the battery could not correctly work. According to the Raman spectra in Fig. 4a, the electrolyte with a NaFSI:AN molar ratio of 1:20 contains a large

amount of free (noncoordinating) AN, which decomposes on hard carbon anode at a low potential,[35,49] leading to poor battery performance. For further investigation of SEI on hard carbon anode, the compositions and the chemical states were studied using XPS (see Fig. S6). It was revealed that the carbon concentration derived from the decomposition of AN solvent decreased with increasing NaFSI salt concentration. Moreover, the SEI formation derived from the FSI^- anion was observed at higher concentrations, which is comparable to previous research.[35] The first discharge capacities of cells with the AN-based electrolytes with NaFSI:AN molar ratios of =1:1, 1:2, 1:2.7, and 1:8 were 144, 184, 192, and 133 mAh g^{-1}, resulting in coulombic efficiencies of 49 %, 56 %, 55 %, and 41 %, respectively. The discharge capacities and coulombic efficiencies of the OSIBs are shown in Fig. 5b. Although the 10th discharge capacity of the cell with the HCE with a NaFSI:AN molar ratio of 1:20 was lower than 3 mAh g^{-1}, the 10th discharge capacities of the cells with HCEs with NaFSI:AN molar ratios of 1:1, 1:2, 1:2.7, and 1:8 were 80, 148, 150, and 74 mAh g^{-1}, resulting in coulombic efficiencies of 91%, 96%, 96%, and 90%, respectively. These results reveal that cells with HCEs with NaFSI:AN molar ratios of 1:2 and 1:2.7 have higher capacities and cycling retention ratio than other cells.

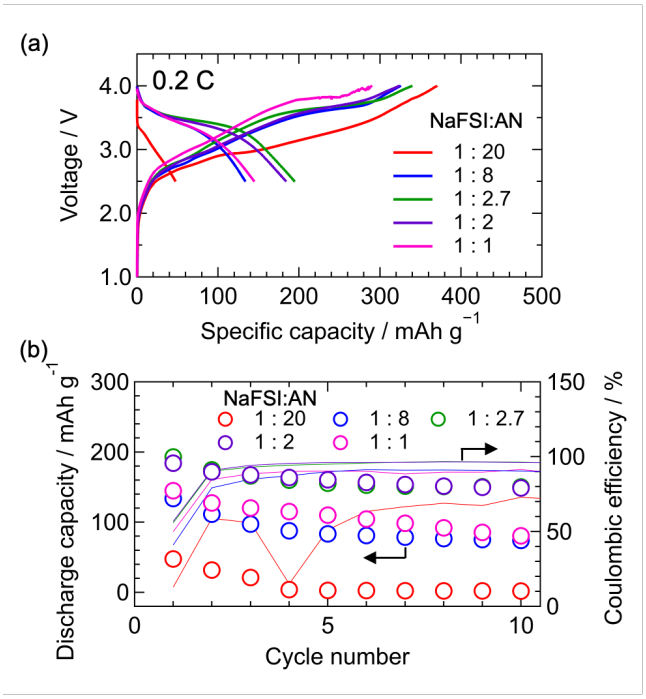

Figure 5. (a) First charge/discharge profiles and (b) cycling properties of organic sodium-ion batteries using a sodium croconate cathode with AN-based electrolytes (NaFSI:AN molar ratios = 1:1, 1:2, 1:2.7, 1:8, and 1:20) at 25°C.

To further investigate the correlation between the cycling property and solution structure of the AN-based HCEs, their 10th discharge capacity retention ratios and 1st coulombic efficiencies were summarized in Fig. 6a, and the fractions of AN and FSI^- anion solvate species were plotted in Fig. 6b and 6c. The fraction of each solvate species was calculated from the area ratios in the deconvoluted Raman spectra (see Fig. 4). First coulombic efficiencies indicated from 40% to 60%, which is comparable to the $C_5O_5Na_2$-based OSIBs with carbonate-based electrolyte (see Fig. S5). For the first cycled carbonate-based electrolytes, a ^{13}C-NMR peak was observed at approximately 184 ppm, which is derived from C_5O_5 molecules (see Fig. S7); the dissolution of C_5O_5 molecules is one of the reasons behind the lower coulombic efficiency and cycling performance of $C_5O_5Na_2$-based OSIBs. For the AN-based HCEs studied in the present work, we considered that C_5O_5 molecules also dissolve into the electrolytes, leading to low coulombic efficiency and poor cycling performance. The cycling retention ratio and coulombic efficiency increased with increasing salt concentration, reaching 80% and 56%, respectively, for the cell with the HCE with a NaFSI:AN molar ratio of 1:2, which has almost no free AN solvent (see Fig. 6b). Nazar *et al.* reported that a very low fraction of free solvent was beneficial in inhibiting the dissolution of active materials into the electrolytes, improving the battery performance of lithium-sulfur batteries.[50] It is considered that the cycling performance of organic batteries would also be improved by reducing the amount of free AN available to solvate the organic molecules. The carbonate-based electrolyte $NaPF_6$/PC, which is generally used in SIBs, also showed a similar tendency, and its cycling retention ratio improved with decreasing free PC (see Fig. S8). By contrast, increasing salt concentration (NaFSI:AN molar ratio = 1:1) decreased the capacity retention ratio and first coulombic efficiency to 55% and 49%, respectively. To confirm the dissolution behavior of organic cathode, separators after 1st charge/discharge measurement were observed (see Fig. S9), and a deep yellow color was observed at higher NaFSI concentration (NaFSI:AN molar ratio = 1:1, see Fig. S9d). Based on the results of the solvate species of the NaFSI/AN-based electrolyte with a molar ratio of 1:1, the fraction of AGG-II structures drastically increased to 60% despite the absence of free solvent (see Fig. 6c), implying that the AGG-II structures, which can affect the solubility of croconates, is detrimental to the cycling performance of the organic batteries.

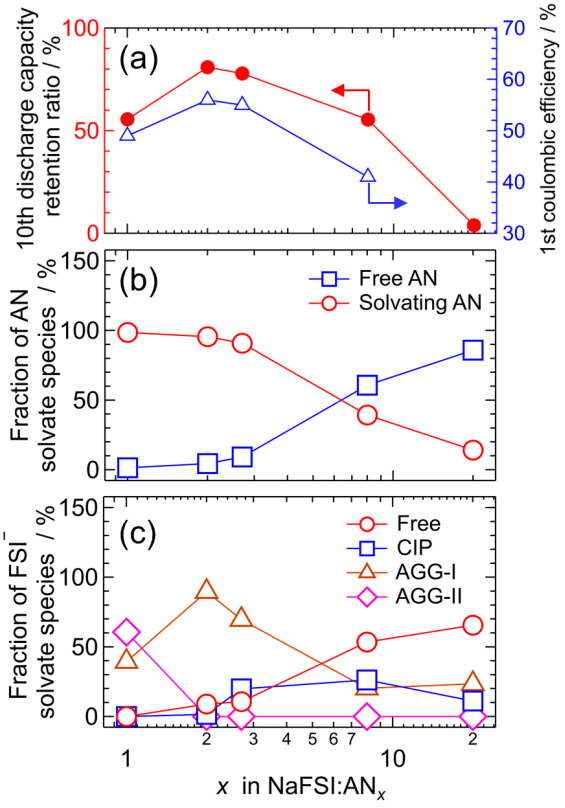

Figure 6. (a) 10th discharge capacity retention ratio and 1st coulombic efficiency of organic sodium-ion batteries with a sodium croconate cathode and the AN-based electrolytes (NaFSI:AN molar ratios = 1:1, 1:2, 1:2.7, 1:8, and 1:20). Fractions of (b) AN solvate species and (c) FSI anion solvate species calculated from the area ratios in the deconvoluted Raman spectra.

Finally, to examine the reaction kinetics between the developed AN-based HCEs and $C_5O_5Na_2$ cathode, we evaluated the C-rate properties of the OSIBs (see Fig. 7a). The cells with the AN-based HCE revealed higher C-rate properties than those with carbonate-based electrolytes (saturated $NaPF_6$ PC) and NaFSI-based HCEs with DME and PC. The first discharge capacity of the cell with the HCE with a NaFSI:AN molar ratio of 1:2.7 was 117 mAh g^{-1} at an even higher C-rate of 10 C. The AN-based HCE also demonstrated better cycling stability than carbonate- and ether-based HCEs (see Fig. 7b). HCE has been reported to have a unique ion transport features, such as a high ion transference number,[34,51] although an increase in salt concentration generally increases its viscosity, leading to lower ionic conductivity. Ionic conductivities of NaFSI:DME (molar ratio = 1:2.7) and NaFSI:PC (molar ratio = 1:2.7) were as high as 7.0 and 2.4 mS cm^{-1} , respectively, at 25 °C (see Fig. S10). Compared with the HCE reported in previous studies, the HCE with a NaFSI:AN molar ratio of 1:2.7 developed in this study had a higher ionic conductivity and t_{Na+} (summarized in Table S4), resulting in cells exhibiting excellent C-rate properties. The 100th discharge capacity of a cell with the HCE with a NaFSI:AN molar ratio of 1:2.7 was 64 mAh g^{-1} at a C-rate of 10 C (see Fig. 7c), resulting in a higher capacity retention ratio of 55% and successful reversible redox reaction at higher C-rates than those observed in carbonate-based electrolytes and NaFSI-based HCEs with DME and PC. Besides the unique high-power performance of OSIBs, the specific capacities and average voltages of the OSIBs are compared with those of state-of-the-art SIB systems in Fig. S11. The performance of the batteries in this study was superior to that of other SIB cathodes, such as those made from transition-metal oxides, polyanion-type compounds, and organic molecules. Moreover, the energy density of the $C_5O_5Na_2$/AN-based HCE/hard carbon SIB system was higher than that of the $LiCoO_2$ cathode used in commercial LIBs. This study provides significant insights into a completely rare-metal (cobalt)-free energy storage system as an alternative to commercial LIBs.

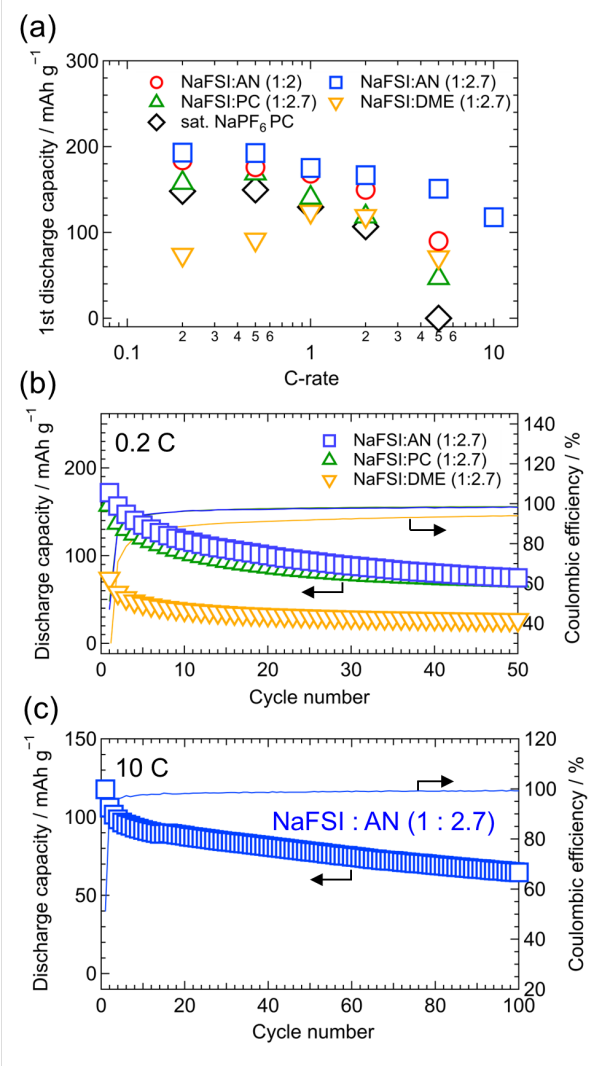

Figure 7. (a) C-rate property of $C_5O_5Na_2$-based organic sodium-ion batteries with NaFSI:AN (molar ratios = 1:2 and 1:2.7), NaFSI:PC (molar ratio = 1:2.7), NaFSI:DME (molar ratio = 1:2.7) and sat. $NaPF_6$ PC as electrolytes at 25°C. (b) Cycling properties of the $C_5O_5Na_2$-based organic sodium-ion batteries with FSI-based HCEs at C-rate of 0.2 C. (c) Cycling properties of $C_5O_5Na_2$-based organic sodium-ion batteries with NaFSI:AN (molar ratio = 1:2.7) at a C-rate of 10 C and 25°C.

CONCLUSIONS

In summary, we demonstrated an AN-based HCE with NaFSI salt. The developed electrolyte with a NaFSI:AN molar ratio of 1:2.7 exhibited an ionic conductivity and t_{Na+} as high as 12.1 mS cm^{-1} and 0.49, respectively. The excellent ion transport property of the electrolyte endowed OSIBs bearing a $C_5O_5Na_2$ cathode and hard carbon anode with higher C-rate properties. We also evaluated the correlation between the solution structure of the HCE and performance of OSIBs bearing a $C_5O_5Na_2$ cathode. The cycling property of the OSIBs improved with increasing salt concentration, and a correlation between the capacity retention ratio and amount of free AN was clearly observed. The cycling property of the OSIBs improved with decreasing free solvent availability owing to the suppression of the dissolution of organic molecules. By contrast, increasing the salt concentration (NaFSI:AN molar ratio = 1:1) decreased the cycling retention ratio, implying that AGG-II structures by FSI^- anions are undesirable to cycling performance. We believe that the above insights will be beneficial for further improvements in the performance of OSIBs and the development of high-power density energy storage systems.

ASSOCIATED CONTENT

Supporting Information

The Supporting Information is available free of charge on the ACS Publications website.

Fitted parameters; electrochemical tests using other electrolytes; thermogravimetric analysis, comparisons with previous research (PDF)

AUTHOR INFORMATION

Corresponding Author

Hiroaki Kobayashi – Department of Chemistry, Faculty of Science, Hokkaido University, Sapporo 060-0810, Japan; orcid.org/0000-0001-6705-9515; E-mail: h.kobayashi@sci.hokudai.ac.jp

Itaru Honma – Institute of Multidisciplinary Research for Advanced Materials, Tohoku University, Sendai 980-8577, Japan; orcid.org/0000-0002-6536-576X; E-mail: itaru.homma.e8@tohoku.ac.jp

Author Contributions

Y. G.: Investigation, Formal analysis, Data curation, Conceptualization, Methodology, Writing – original draft; H. K.: Supervision, Conceptualization, Methodology, Writing – review & editing, Funding acquisition; I. H.: Supervision, Conceptualization, Methodology, Writing – review & editing, Funding acquisition, Project administration.

Notes

The authors declare no competing financial interest.

ACKNOWLEDGMENT

This study was supported by JSPS KAKENHI (Grant Number 21H04696), and the Cooperative Research Program of NJRC Mater. & Dev. (MEXT), Japan. Part of this work was supported by the Central Analytical Facility of the Institute of Multidisciplinary Research for Advanced Materials (Tagen CAF), Tohoku University. We also thank Prof. T. Tomai, and Mr. M. Hino for their kind help with the viscosity and the NMR measurement, respectively.

REFERENCES

(1) Goodenough, J. B.; Park, K. S. The Li-Ion Rechargeable Battery: A Perspective. *J. Am. Chem. Soc.* **2013**, *135*, 1167–1176. https://doi.org/10.1021/ja3091438.

(2) Armand, M. Nature Lithium Battery. *Nature* **2001**, *414*, 359–367.

(3) Sun, X.; Hao, H.; Hartmann, P.; Liu, Z.; Zhao, F. Supply Risks of Lithium-Ion Battery Materials: An Entire Supply Chain Estimation. *Mater. Today Energy* **2019**, *14*, 100347. https://doi.org/10.1016/j.mtener.2019.100347.

(4) Chen, H.; Armand, M.; Demailly, G.; Dolhem, F.; Poizot, P.; Tarascon, J. M. From Biomass to a Renewable $LiXC_6O_6$ Organic Electrode for Sustainable Li-Ion Batteries. *ChemSusChem* **2008**, *1*, 348–355. https://doi.org/10.1002/cssc.200700161.

(5) Liang, Y.; Yao, Y. Positioning Organic Electrode Materials in the Battery Landscape. *Joule* **2018**, *2*, 1690–1706. https://doi.org/10.1016/j.joule.2018.07.008.

(6) Lyu, H.; Jafta, C. J.; Popovs, I.; Meyer, H. M.; Hachtel, J. A.; Huang, J.; Sumpter, B. G.; Dai, S.; Sun, X. G. A Dicyanobenzoquinone Based Cathode Material for Rechargeable Lithium and Sodium Ion Batteries. *J. Mater. Chem. A* **2019**, *7*, 17888–17895. https://doi.org/10.1039/c9ta04869c.

(7) Tomai, T.; Saito, H.; Honma, I. High-Energy-Density Electrochemical Flow Capacitors Containing Quinone Derivatives Impregnated in Nanoporous Carbon Beads. *J. Mater. Chem. A* **2017**, *5*, 2188–2194. https://doi.org/10.1039/C6TA08733G.

(8) Wang, X.; Shang, Z.; Yang, A.; Zhang, Q.; Cheng, F.; Jia, D.; Chen, J. Combining Quinone Cathode and Ionic Liquid Electrolyte for Organic Sodium-Ion Batteries. *Chem* **2019**, *5*, 364–375. https://doi.org/10.1016/j.chempr.2018.10.018.

(9) Son, E. J.; Kim, J. H.; Kim, K.; Park, C. B. Quinone and Its Derivatives for Energy Harvesting and Storage Materials. *J. Mater. Chem. A* **2016**, *4*, 11179–11202. https://doi.org/10.1039/c6ta03123d.

(10) Sieuw, L.; Jouhara, A.; Quarez, É.; Auger, C.; Gohy, J. F.; Poizot, P.; Vlad, A. A H-Bond Stabilized Quinone Electrode Material for Li-Organic Batteries: The Strength of Weak Bonds. *Chem. Sci.* **2019**, *10*, 418–426. https://doi.org/10.1039/c8sc02995d.

(11) Zheng, S.; Hu, J.; Huang, W. An Inorganic-Organic Nanocomposite Calix[4]Quinone (C4Q)/CMK-3 as a Cathode Material for High-Capacity Sodium Batteries. *Inorg. Chem. Front.* **2017**, *4*, 1806–1812. https://doi.org/10.1039/c7qi00453b.

(12) Xiong, W.; Huang, W.; Zhang, M.; Hu, P.; Cui, H.; Zhang, Q. Pillar[5]Quinone-Carbon Nanocomposites as High-Capacity Cathodes for Sodium-Ion Batteries. *Chem. Mater.* **2019**, *31*, 8069–8075. https://doi.org/10.1021/acs.chemmater.9b02601.

(13) Katsuyama, Y.; Kobayashi, H.; Iwase, K.; Gambe, Y.; Honma, I. Are Redox-Active Organic Small Molecules Applicable for High-Voltage (>4 V) Lithium-Ion Battery Cathodes? *Adv. Sci.* **2022**, *9*, 2200187. https://doi.org/10.1002/advs.202200187.

(14) Fujihara, Y.; Fujihara, Y.; Kobayashi, H.; Takaishi, S.; Tomai, T.; Yamashita, M.; Yamashita, M.; Yamashita, M.; Honma, I. Electrical Conductivity-Relay between Organic Charge-Transfer and Radical Salts toward Conductive Additive-Free Rechargeable Battery. *ACS Appl. Mater. Interfaces* **2020**, *12*, 25748–25755. https://doi.org/10.1021/acsami.0c03642.

(15) Chihara, K.; Chujo, N.; Kitajou, A.; Okada, S. Cathode Properties of $Na_2C_6O_6$ for Sodium-Ion Batteries. *Electrochim. Acta* **2013**, *110*, 240–246. https://doi.org/10.1016/j.electacta.2013.04.100.

(16) Luo, C.; Fan, X.; Ma, Z.; Gao, T.; Wang, C. Self-Healing Chemistry between Organic Material and Binder for Stable Sodium-Ion Batteries. *Chem* **2017**, *3*, 1050–1062. https://doi.org/10.1016/j.chempr.2017.09.004.

(17) Wang, C.; Fang, Y.; Xu, Y.; Liang, L.; Zhou, M.; Zhao, H.; Lei, Y. Manipulation of Disodium Rhodizonate: Factors for Fast-Charge and Fast-Discharge Sodium-Ion Batteries with Long-

Term Cyclability. *Adv. Funct. Mater.* **2016**, *26*, 1777–1786. https://doi.org/10.1002/adfm.201504537.

(18) Hanyu, Y.; Honma, I. Rechargeable Quasi-Solid State Lithium Battery with Organic Crystalline Cathode. *Sci. Rep.* **2012**, *2*, 453. https://doi.org/10.1038/srep00453.

(19) Hanyu, Y.; Ganbe, Y.; Honma, I. Application of Quinonic Cathode Compounds for Quasi-Solid Lithium Batteries. *J. Power Sources* **2013**, *221*, 186–190. https://doi.org/10.1016/j.jpowsour.2012.08.040.

(20) Hanyu, Y.; Sugimoto, T.; Ganbe, Y.; Masuda, A.; Honma, I. Multielectron Redox Compounds for Organic Cathode Quasi-Solid State Lithium Battery. *J. Electrochem. Soc.* **2014**, *161*, A6–A9. https://doi.org/10.1149/2.015401jes.

(21) Yao, M.; Kuratani, K.; Kojima, T.; Takeichi, N.; Senoh, H.; Kiyobayashi, T. Indigo Carmine: An Organic Crystal as a Positive-Electrode Material for Rechargeable Sodium Batteries. *Sci. Rep.* **2014**, *4*, 3650. https://doi.org/10.1038/srep03650.

(22) Gambe, Y.; Kobayashi, H.; Honma, I. A 3.5 V-Class Organic Sodium-Ion Battery Using a Croconate Cathode. *Chem. Eng. J.* **2024**, *479*, 147760. https://doi.org/10.1016/j.cej.2023.147760.

(23) Kim, J. K.; Kim, Y.; Park, S.; Ko, H.; Kim, Y. Encapsulation of Organic Active Materials in Carbon Nanotubes for Application to High-Electrochemical-Performance Sodium Batteries. *Energy Environ. Sci.* **2016**, *9*, 1264–1269. https://doi.org/10.1039/c5ee02806j.

(24) Xu, F.; Xia, J.; Shi, W.; Cao, S. A. Sulfonyl-Based Polyimide Cathode for Lithium and Sodium Secondary Batteries: Enhancing the Cycling Performance by the Electrolyte. *Mater. Chem. Phys.* **2016**, *169*, 192–197. https://doi.org/10.1016/j.matchemphys.2015.12.004.

(25) Zhong, H.; Wang, G.; Song, Z.; Li, X.; Tang, H.; Zhou, Y.; Zhan, H. Organometallic Polymer Material for Energy Storage. *Chem. Commun.* **2014**, *50*, 6768–6770. https://doi.org/10.1039/c4cc01572j.

(26) Mao, M.; Luo, C.; Pollard, T. P.; Hou, S.; Gao, T.; Fan, X.; Cui, C.; Yue, J.; Tong, Y.; Yang, G.; Deng, T.; Zhang, M.; Ma, J.; Suo, L.; Borodin, O.; Wang, C. A Pyrazine-Based Polymer for Fast-Charge Batteries. *Angew. Chemie - Int. Ed.* **2019**, *58*, 17820–17826. https://doi.org/10.1002/anie.201910916.

(27) Zhou, M.; Xiong, Y.; Cao, Y.; Ai, X.; Yang, H. Electroactive Organic Anion-Doped Polypyrrole as a Low Cost and Renewable Cathode for Sodium-Ion Batteries. *J. Polym. Sci. Part B Polym. Phys.* **2013**, *51*, 114–118. https://doi.org/10.1002/polb.23184.

(28) Aztatzi-Pluma, D.; Castrejón-González, E. O.; Almendarez-Camarillo, A.; Alvarado, J. F. J.; Durán-Morales, Y. Study of the Molecular Interactions between Functionalized Carbon Nanotubes and Chitosan. *J. Phys. Chem. C* **2016**, *120*, 2371–2378. https://doi.org/10.1021/acs.jpcc.5b08136.

(29) Unemoto, A.; Gambe, Y.; Komatsu, D.; Honma, I. Development of High Capacity All-Solid-State Lithium Battery Using Quasi-Solid-State Electrolyte Containing Tetraglyme-Li-TFSA Equimolar Complexes. *Solid State Ionics* **2014**, *262*, 765–768. https://doi.org/10.1016/j.ssi.2013.09.043.

(30) Song, Z.; Qian, Y.; Zhang, T.; Otani, M.; Zhou, H. Poly(Benzoquinonyl Sulfide) as a High-Energy Organic Cathode for Rechargeable Li and Na Batteries. *Adv. Sci.* **2015**, *2*, 1–9. https://doi.org/10.1002/advs.201500124.

(31) Li, A.; Feng, Z.; Sun, Y.; Shang, L.; Xu, L. Porous Organic Polymer/RGO Composite as High Performance Cathode for Half and Full Sodium Ion Batteries. *J. Power Sources* **2017**, *343*, 424–430. https://doi.org/10.1016/j.jpowsour.2017.01.079.

(32) Su, C.; He, H.; Xu, L.; Zhao, K.; Zheng, C.; Zhang, C. A Mesoporous Conjugated Polymer Based on a High Free Radical Density Polytriphenylamine Derivative: Its Preparation and Electrochemical Performance as a Cathode Material for Li-Ion Batteries. *J. Mater. Chem. A* **2017**, *5*, 2701–2709. https://doi.org/10.1039/c6ta10127e.

(33) Yamada, Y. Developing New Functionalities of Superconcentrated Electrolytes for Lithium-Ion Batteries. *Electrochemistry* **2017**, *85*, 559–565. https://doi.org/10.5796/electrochemistry.85.559.

(34) Okamoto, Y.; Tsuzuki, S.; Tatara, R.; Ueno, K.; Dokko, K.; Watanabe, M. High Transference Number of Na Ion in Liquid-State Sulfolane Solvates of Sodium Bis(Fluorosulfonyl)Amide. *J. Phys. Chem. C* **2020**, *124*, 4459–4469. https://doi.org/10.1021/acs.jpcc.9b11458.

(35) Takada, K.; Yamada, Y.; Watanabe, E.; Wang, J.; Sodeyama, K.; Tateyama, Y.; Hirata, K.; Kawase, T.; Yamada, A. Unusual Passivation Ability of Superconcentrated Electrolytes toward Hard Carbon Negative Electrodes in Sodium-Ion Batteries. *ACS Appl. Mater. Interfaces* **2017**, *9*, 33802–33809. https://doi.org/10.1021/acsami.7b08414.

(36) Kim, J. M.; Gao, P.; Miao, Q.; Zhao, Q.; Rahman, M. M.; Chen, P.; Zhang, X.; Hu, E.; Liu, P.; Zhang, J. G.; Xu, W. Tailoring Solvation Solvent in Localized High-Concentration Electrolytes for Lithium||Sulfurized Polyacrylonitrile. *ACS Appl. Mater. Interfaces* **2024**, 16, 20618-20625. https://doi.org/10.1021/acsami.4c02326.

(37) Chen, X.; Meng, Y.; Xiao, D.; Wu, Y.; Qin, L. Tunning Solvation Structure in Non-Flammable, Localized High-Concentration Electrolytes with Enhanced Stability towards All Aluminum Substrate-Based K Batteries. *Energy Storage Mater.* **2023**, *61* 102923. https://doi.org/10.1016/j.ensm.2023.102923.

(38) Qin, L.; Xiao, N.; Zheng, J.; Lei, Y.; Zhai, D.; Wu, Y. Localized High-Concentration Electrolytes Boost Potassium Storage in High-Loading Graphite. *Adv. Energy Mater.* **2019**, *9*, 1902618. https://doi.org/10.1002/aenm.201902618.

(39) Li, M.; Liu, Y.; Yang, X.; Zhang, Q.; Cheng, Y.; Deng, L.; Zhou, Q.; Cheng, T.; Gu, M. D. Acetonitrile-Based Local High-Concentration Electrolytes for Advanced Lithium Metal Batteries. *Adv. Mater.* **2024**, *36*, 2404271. https://doi.org/10.1002/adma.202404271.

(40) Guo, C.; Zhang, K.; Zhao, Q.; Pei, L.; Chen, J. High-Performance Sodium Batteries with the 9,10-Anthraquinone/CMK-3 Cathode and an Ether-Based Electrolyte. *Chem. Commun.* **2015**, *51*, 10244–10247. https://doi.org/10.1039/c5cc02251g.

(41) Li, M.; Hicks, R. P.; Chen, Z.; Luo, C.; Guo, J.; Wang, C.; Xu, Y. Electrolytes in Organic Batteries. *Chem. Rev.* **2023**, 123, 1712-1773. https://doi.org/10.1021/acs.chemrev.2c00374.

(42) Ugata, Y.; Thomas, M. L.; Mandai, T.; Ueno, K.; Dokko, K.; Watanabe, M. Li-Ion Hopping Conduction in Highly Concentrated Lithium Bis(Fluorosulfonyl)Amide/Dinitrile Liquid Electrolytes. *Phys. Chem. Chem. Phys.* **2019**, *21*, 9759–9768. https://doi.org/10.1039/c9cp01839e.

(43) Ugata, Y.; Tatara, R.; Ueno, K.; Dokko, K.; Watanabe, M. Highly Concentrated LiN(SO2CF3)2/Dinitrile Electrolytes: Liquid Structures, Transport Properties, and Electrochemistry. *J. Chem. Phys.* **2020**, *152*, 104502. https://doi.org/10.1063/1.5145340.

(44) Morales, D.; Chagas, L. G.; Paterno, D.; Greenbaum, S.; Passerini, S.; Suarez, S. Transport Studies of NaPF6 Carbonate Solvents-Based Sodium Ion Electrolytes. *Electrochim. Acta* **2021**, *377*, 138062. https://doi.org/10.1016/j.electacta.2021.138062.

(45) Yoshida, K.; Tsuchiya, M.; Tachikawa, N.; Dokko, K.; Watanabe, M. Change from Glyme Solutions to Quasi-Ionic Liquids for Binary Mixtures Consisting of Lithium Bis(Trifluoromethanesulfonyl)Amide and Glymes. *J. Phys. Chem. C* **2011**, *115*, 18384–18394. https://doi.org/10.1021/jp206881t.

(46) Evans, J.; Vincent, C. A.; Bruce, P. G. Electrochemical Measurement of Transference Numbers in Polymer Electrolytes. *Polymer (Guildf).* **1987**, *28*, 2324–2328. https://doi.org/10.1016/0032-3861(87)90394-6.

(47) Dokko, K.; Watanabe, D.; Ugata, Y.; Thomas, M. L.; Tsuzuki, S.; Shinoda, W.; Hashimoto, K.; Ueno, K.; Umebayashi, Y.; Watanabe, M. Direct Evidence for Li Ion Hopping Conduction in Highly Concentrated Sulfolane-Based Liquid Electrolytes. *J. Phys. Chem. B* **2018**, *122*, 10736–10745. https://doi.org/10.1021/acs.jpcb.8b09439.

(48) Seo, D. M.; Borodin, O.; Han, S.-D.; Boyle, P. D.; Henderson, W. A. Electrolyte Solvation and Ionic Association II. Acetonitrile-Lithium Salt Mixtures: Highly Dissociated Salts. *J. Electrochem.*

Soc. **2012**, *159*, A1489–A1500. https://doi.org/10.1149/2.035209jes.

(49) Yamada, Y.; Furukawa, K.; Sodeyama, K.; Kikuchi, K.; Yaegashi, M.; Tateyama, Y.; Yamada, A. Unusual Stability of Acetonitrile-Based Superconcentrated Electrolytes for Fast-Charging Lithium-Ion Batteries. *J. Am. Chem. Soc.* **2014**, *136*, 5039–5046. https://doi.org/10.1021/ja412807w.

(50) Cuisinier, M.; Cabelguen, P. E.; Adams, B. D.; Garsuch, A.; Balasubramanian, M.; Nazar, L. F. Unique Behaviour of Nonsolvents for Polysulphides in Lithium-Sulphur Batteries. *Energy Environ. Sci.* **2014**, *7*, 2697–2705. https://doi.org/10.1039/c4ee00372a.

(51) Ugata, Y.; Thomas, M. L.; Mandai, T.; Ueno, K.; Dokko, K.; Watanabe, M. Li-Ion Hopping Conduction in Highly Concentrated Lithium Bis(Fluorosulfonyl)Amide/Dinitrile Liquid Electrolytes. *Phys. Chem. Chem. Phys.* **2019**, *21*, 9759–9768. https://doi.org/10.1039/c9cp01839e.